



Sejdinovic, D., Ponnampalam, V., Piechocki, R. J., & Doufexi, A. (2008). The throughput analysis of different IR-HARQ schemes based on fountain codes. In IEEE Wireless Communications and Networking Conference 2008, Las Vegas. (pp. 267 - 272). Institute of Electrical and Electronics Engineers (IEEE). doi: 10.1109/WCNC.2008.52, 10.1109/WCNC.2008.52

Link to published version (if available):

doi: [10.1109/WCNC.2008.52](https://doi.org/10.1109/WCNC.2008.52)
[10.1109/WCNC.2008.52](https://doi.org/10.1109/WCNC.2008.52)

[Link to publication record in Explore Bristol Research](#)

PDF-document

University of Bristol - Explore Bristol Research

General rights

This document is made available in accordance with publisher policies. Please cite only the published version using the reference above. Full terms of use are available:
<http://www.bristol.ac.uk/pure/about/ebr-terms.html>

Take down policy

Explore Bristol Research is a digital archive and the intention is that deposited content should not be removed. However, if you believe that this version of the work breaches copyright law please contact open-access@bristol.ac.uk and include the following information in your message:

- Your contact details
- Bibliographic details for the item, including a URL
- An outline of the nature of the complaint

On receipt of your message the Open Access Team will immediately investigate your claim, make an initial judgement of the validity of the claim and, where appropriate, withdraw the item in question from public view.

The throughput analysis of different IR-HARQ schemes based on fountain codes

Dino Sejdinović*, Vishakan Ponnampalam†, Robert J. Piechocki* and Angela Doufexi*

*Centre for Communications Research

Department of Electrical & Electronic Engineering

University of Bristol, Bristol, UK

{d.sejdinovic, r.j.piechocki, a.doufexi}@bristol.ac.uk

†Toshiba Research Europe Ltd

Telecommunications Research Laboratory

32 Queen Square, Bristol, UK

vishakan.ponnampalam@toshiba-trel.com

Abstract—In this contribution, we construct two novel IR-HARQ schemes based on fountain codes, which combine the punctured and rateless IR-HARQ schemes, in order to attain the advantageous properties of both: nearly optimal performance of the former at the high signal-to-noise ratio (SNR) region and ratelessness of the latter. The preliminary simulation results indicate that these schemes are particularly suitable for scenarios where the transmission is originally assumed to occur at the very high SNR region, but resilience to severe deterioration of channel conditions is required.

I. INTRODUCTION

Reliable error detection in the ARQ (Automatic Repeat reQuest) schemes is provided by Cyclic Redundancy Check (CRC) codes. If a received set of symbols passes the CRC test, the receiver sends an acknowledgment (ACK) of successful reception to the transmitter. Otherwise, the receiver requests retransmission (NAK) and retransmissions proceed until ACK has been received at the transmitter end. Furthermore, the data set may be protected by an additional error correcting code. This increases the probability of successful reception at the cost of decreasing the actual transmission rate. Combination of the principles of FEC (forward error correction) and ARQ gives rise to Hybrid ARQ (HARQ) schemes. The standard measure of HARQ protocol efficiency is its *throughput*, defined as the average number of correctly received data bits accepted at the receiver in the time required for transmission of a single bit. When there is knowledge of the channel conditions, a fixed rate code which is well suited for such channel can be employed. However, in wireless networks and other applications with varying channel conditions, higher throughput is achieved by error correction schemes of varying rate, i.e., schemes which increment redundancy in stages. These schemes are referred to as Incremental Redundancy Hybrid ARQ (IR-HARQ) or type II HARQ schemes [1].

Modification of a standard fixed-rate code in order to make it suitable for the IR-HARQ scheme is usually done by *puncturing*. For example, let us consider the IR-HARQ transmission protocol over a Binary Input Memoryless Symmetric (BIMS) channel. One can encode the input vector,

which is assumed to contain both the information sequence and the CRC bits, with a good systematic LDPC code, which is usually called *mother code*. At the first transmission, the systematic part of the codeword and a selected number of parity symbols are sent. The standard belief propagation (BP) sum-product decoding algorithm can then be performed at the receiver, provided that the log-likelihood ratios of the parity symbols which were not transmitted are initialized to zero (which precisely means that no direct information about corresponding symbols is available). If the decoding fails, retransmission is requested, and after that the transmitter sends set of additional parity symbols from the codeword of the mother code. The procedure is repeated until the decoding is successful and an ACK is received. The research topics associated with such *punctured* IR-HARQ schemes are the design of the mother code and the puncturing schedule. The rate of the mother code and the choice of puncturing schedule determine the throughput of the punctured IR-HARQ scheme. However, due to the finite length of the mother code, there exists a certain noise threshold for each punctured IR-HARQ scheme. When signalling at an SNR lower than this threshold, the decoding success cannot be guaranteed even when the entire codeword has been transmitted. This generally occurs if channel conditions severely deteriorate and mother code rate exceeds channel capacity. When using a simple random puncturing schedule on a standard LDPC mother code, one can note the tradeoff between the random puncturing efficiency and the rate of the mother code - higher rate LDPC codes as mother codes provide very good throughput efficiency at high values of SNR, however their noise threshold is also higher.

In order to guarantee successful decoding even at extremely severe channel conditions, one may either introduce a very low rate mother code with an advanced puncturing technique or start with a high-rate mother code and provide means of its *extending* [2]. Another potential solution arose with the introduction of *rateless* or *digital fountain* (DF) codes [3], [4]. DF codes provide with the framework of generating as many encoding symbols as necessary on the fly, all those symbols being pseudorandom, equally important descriptions

of the source. The analysis and comparison of two schemes, punctured IR-HARQ scheme based on LDPC codes and *rateless* IR-HARQ scheme based on Raptor codes [4] was undertaken in [5]. It has been shown that the punctured scheme performs better on the region of high SNR, i.e., for the region higher than the threshold of the code, while rateless scheme, as expected, works reasonably well on a much wider range of SNR - Raptor codes can be used for signalling at extremely low SNR and still perform near the capacity. It was argued that if the operating region of SNR is guaranteed to be high, punctured IR-HARQ scheme with high rate mother LDPC code performs better, whereas rateless IR-HARQ scheme is more suitable in scenarios with no available information about channel conditions.

In the rest of the paper, we will propose two adaptive techniques which combine the punctured and the rateless approach, with the following scenario in mind. Although no channel state information is available, the transmission is assumed to occur at a high SNR region for most of the transmission sessions, but robust transmission in the case of a sudden and random deterioration of channel conditions is also required. Our design utilizes a high-rate LDPC mother code and proceeds with a standard punctured IR-HARQ scheme in the first stage of transmission. If the decoding does not occur when the entire codeword of the mother code has been transmitted, the rateless IR-HARQ scheme should be employed, but in such a way as to make use of the already transmitted symbols, i.e., both systematic symbols and parities of the mother code. The rationale behind this technique is rather simple. At the high SNR region, one would attain the almost optimal performance of punctured scheme, whereas at the lower SNR region one would benefit from the robustness of the rateless scheme. Two different combined “punctured + rateless” IR-HARQ schemes are presented in sections III and IV, whereas section II reviews the decoding algorithm for Raptor codes and describes the rateless IR-HARQ scheme with Raptor codes. Our combined schemes, referred to as schemes A and B, both proceed with a punctured IR-HARQ scheme in the first stage of transmission but differently approach the problem of how to continue transmission when all the mother code parities have been transmitted and the receiver still cannot decode the information sequence. Scheme A transmits the standard Raptor encoding symbols and modifies the decoding algorithm such that soft information based on the already received symbols can be used, whereas scheme B employs the systematic Raptor design in order to make use of the already transmitted symbols.

II. IR-HARQ BASED ON RAPTOR CODES

Raptor codes are a state-of-the-art DF solution for lossy transmission with excellent performance and linear encoding/decoding complexity, also studied at noisy BIMS channels [6]. To obtain the Raptor encoding symbols, the information sequence of k symbols is pre-coded by a high rate (n, k) -linear code with parity check matrix \mathbf{H} , e.g. a high-rate LDPC code. Raptor encoding symbols are then generated using an LT

(Luby Transform) code [3] with the output degree distribution $\Omega(x) = \sum_{d=1}^n \Omega_d x^d$. After the output degree d is chosen, d input symbols are chosen uniformly at random from the pre-coded information sequence and then XOR-ed to form a Raptor encoding symbol. Each encoding symbol is generated independently, and thus the number of possible encoding symbols is unlimited. Based on the set of received Raptor encoding symbols, the receiver “sees” the generator matrix \mathbf{G}_{LT} of the LT code, because it shares the same pseudorandom number generator with the transmitter. In the IR-HARQ transmission, the receiver attempts decoding at equal intervals of reception and keeps on collecting the Raptor encoding symbols until the decoding is successful.

The belief propagation algorithm for decoding of Raptor codes over BIMS channel consists of two stages. At first, BP decoding on the graph based on the matrix $[\mathbf{H}^T \mathbf{G}_{LT}^T]^T$ is performed for a fixed number of iterations to obtain the approximate log-likelihood ratios (LLRs) of input nodes. Here, every dynamic output node f , i.e., the one corresponding to the Raptor encoding symbol has a corresponding channel LLR $L(z_f)$, derived based on the channel output z_f . Static nodes, i.e., those corresponding to parity check of the precode are instantiated with $L(z_f) = \infty$, since they are deterministically equal to zero. The iterations proceed as follows.

$$\tanh\left(\frac{\mu_{f,v}^{(i)}}{2}\right) = \begin{cases} \tanh\left(\frac{L(z_f)}{2}\right) & , i = 0, \\ \tanh\left(\frac{L(z_f)}{2}\right) \prod_{u \neq v} \tanh\left(\frac{m_{u,f}^{(i-1)}}{2}\right) & , i \geq 1. \end{cases} \quad (1)$$

$$m_{v,f}^{(i)} = \sum_{g \neq f} \mu_{g,v}^{(i)}, \quad i \geq 0, \quad (2)$$

where $\mu_{f,v}^{(i)}$ ($m_{v,f}^{(i)}$) are the messages passed from the output node f to the input node v (from the input node v to the output node f) at the i -th iteration.

After a fixed number of iterations l , the LLR of the input node v are given by

$$L(y_v) = \sum_g \mu_{g,v}^{(l)}. \quad (3)$$

These LLRs are gathered and used as prior LLRs of the input nodes on the static decoding graph of the Raptor code, i.e., the decoding graph of the precode.

III. COMBINED IR-HARQ SCHEME A: USING SOFT INFORMATION AT THE INPUT NODES

One way to think about the IR-HARQ scheme is to put it into the context of distributed joint source-channel coding (DJSCC) and to perform decoding by employing soft information about both input and output nodes. The ideas of using Raptor codes for DJSCC as well as the Raptor decoding algorithm with soft information at the input nodes were explored in [7]. After the decoding of the mother LDPC code fails, which is also the precode of the Raptor code, Raptor encoding symbols may be transmitted as additional parities, containing soft information based on the channel output. The

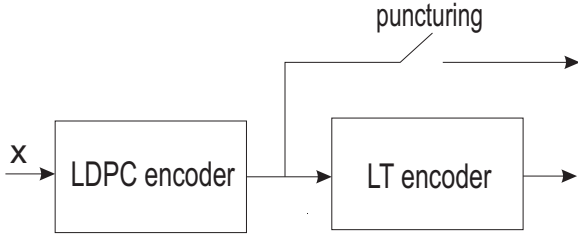


Fig. 1. Block diagram for the encoder for combined scheme A

block diagram for this scheme is also depicted in 1. The nodes corresponding to the Raptor encoding symbols are embedded into the decoding graph of the mother LDPC code. This is a more general version of belief propagation, since soft information is present at both sides of the graph. It is given by

$$m_{v,f}^{(i)} = \begin{cases} L(y_v) & , i = 0, \\ L(y_v) + \sum_{g \neq f} \mu_{g,v}^{(i-1)} & , i \geq 1. \end{cases} \quad (4)$$

$$\tanh\left(\frac{\mu_{f,v}^{(i)}}{2}\right) = \tanh\left(\frac{L(z_f)}{2}\right) \prod_{u \neq v} \tanh\left(\frac{m_{u,f}^{(i)}}{2}\right), \quad i \geq 0, \quad (5)$$

where notation is as in the previous section and $L(y_v)$ are the log-likelihood ratios of the received systematic symbols and mother code parities.

The difference between our case and scenario from [7] is that parity nodes also contain soft information since they have been transmitted through the channel for the purposes of the first part of the protocol, i.e., LDPC decoding. Hence, in this scenario there is no need for *bias* towards the parity symbols in forming of the Raptor encoding symbols, which was introduced in [7]. Again, we have $L(z_f) = \infty$ where f is the parity check node of the precode.

In Fig. 2, the graph used for BP decoding in combined scheme A is presented. The input nodes are on the left side, white nodes correspond to the systematic symbols, whereas dark ones correspond to the parity symbols. Soft information based on channel output about both systematic and parity symbols is available, since the entire codeword of the mother code has been transmitted during the first stage of the IR-HARQ scheme. On the right side, squares are parity-check nodes of the mother code (precode), and shaded nodes correspond to the Raptor encoding symbols. The Raptor encoding symbols also contain the soft information based on the channel output.

The simulation results and comparison of combined IR-HARQ scheme A with the corresponding rateless IR-HARQ with Raptor code and punctured high-rate LDPC IR-HARQ schemes over the BIAWGN (Binary Input Additive White Gaussian Noise) channel are presented in Fig. 3. The channel metric is in terms of signal-to-noise ratio (SNR): $\text{SNR} = 10 \log_{10} \frac{1}{\sigma^2}$ where σ^2 is the channel noise variance. After the reception of systematic symbols, decoding is attempted at equal intervals. Each time decoding fails, additional set of encoding symbols is transmitted. Throughput is calculated as

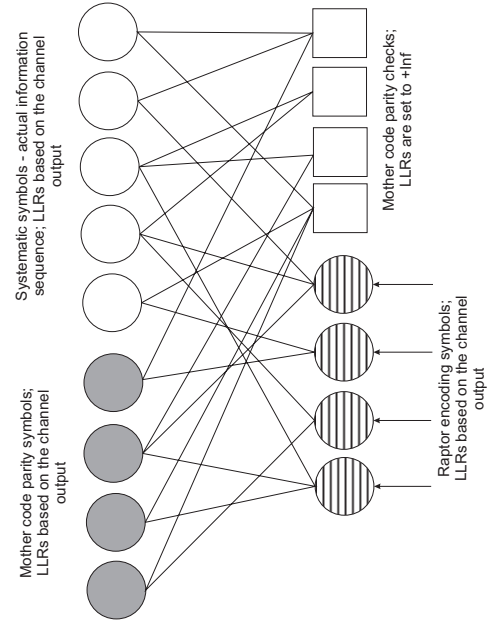


Fig. 2. Decoding graph for combined scheme A

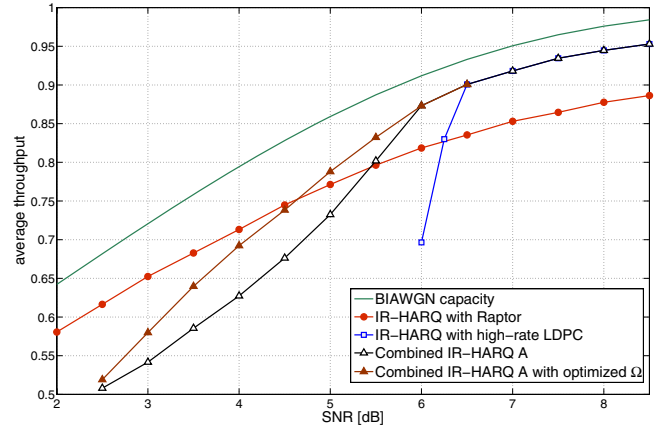


Fig. 3. Simulation results for combined scheme A

the average data rate at which decoding attempt succeeds. In our simulation scenario, we have considered an information sequence of $k = 3140$ bits. The pre-code used was an LDPC code constructed by MacKay [8]. The output degree distribution we used was the same as the one used in [5]. Noticeable advantage of the combined scheme A over rateless IR-HARQ with Raptor code exists at the region of high SNR, since the combined scheme successfully takes advantage of the first stage of the transmission, i.e., puncturing of LDPC mother code. However, Raptor IR-HARQ still significantly outperforms the combined scheme A at the region of low SNR.

The optimization of fountain code output symbol degree distribution for the BIAWGN channel when soft information is not present at the input nodes was treated in [6] by using a refined Gaussian approximation [9]. This optimization is based on the simple rationale. Under the usual all-zeroes information sequence assumption, the means of the messages

transmitted from the input nodes to the output nodes during the sum-product algorithm should keep on increasing up to a certain predefined value μ_{max} . The linear program used for optimization thus carries the constraints

$$\alpha \sum_d \omega_d f_d(\mu) > \mu, \mu \in (0, \mu_{max}) \quad (6)$$

where $\omega(x) = \frac{\Omega'(x)}{\Omega'(1)}$ is the output edge degree distribution (the proportion of incoming messages with the mean $f_d(\mu)$), α is the average input degree and $f_d(\mu)$ is the refined mean [6] of the messages passed from the output node of degree d when the mean of the incoming messages is μ .

Note that the absence of the soft information implies that the starting mean of the messages sent from the input nodes to the output nodes has to be zero. However, in the case when there is soft information available also at the input nodes, the constraints imposed by (6) are more strict than it is necessary. If we assume that the information sequence is an all-zeroes message, then presence of already transmitted systematic symbols induces that the mean of the messages sent from the input nodes to the output nodes at the first iteration of the message-passing algorithm is $\mu_0 = 2/\sigma^2$, where σ^2 is the noise variance of the BIAWGN channel through which systematic symbols have been transmitted. Hence, means should keep on increasing only on the interval (μ_0, μ_{max}) . Also, the input node-update is now different since it needs to take intrinsic soft information into account. The new “mean-increase” condition becomes:

$$\mu_0 + \alpha \sum_d \omega_d f_d(\mu) > \mu, \mu \in (\mu_0, \mu_{max}). \quad (7)$$

Using this modified optimization procedure we were able to obtain different output symbol degree distributions Ω , which take into account the fact that systematic symbols have already been transmitted during the first part of the scheme. In Fig. 2, the simulation results for the distribution Ω optimized for an SNR of 4 dB are presented. We note that the combined scheme A with this optimized distribution further enhances the performance, however it starts failing at the region of lower SNR. This is because the linear constraints in the described optimization procedure become too weak as the SNR decreases.

The advantage of this approach in comparison to IR-HARQ based on Raptor codes only, apart from the enhanced performance at the high SNR region, is lower computational complexity of the decoding procedure. Namely, the decoding is done on a graph of considerably smaller size. The decoding graph for the rateless IR-HARQ scheme based on Raptor codes as in our simulation scenario requires the decoding graph with 3583 input nodes (both systematic and parity symbols) and the average of 4658 output nodes (including both parity checks and Raptor encoding symbols) to correctly recover the information sequence at an SNR of 4.5 dB. On the other hand, the decoding graph of the combined scheme, due to the presence of soft information at the input nodes, requires only an average of 1503 output nodes for the same value of

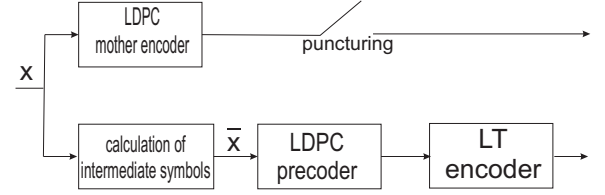


Fig. 4. Block diagram for the encoder for combined scheme B

SNR. This implies that more than three times fewer edges in the decoding graph are to be processed during the sum-product algorithm.

IV. COMBINED IR-HARQ SCHEME B: EMPLOYING SYSTEMATIC RAPTOR DESIGN

Another way to achieve the combination of punctured and rateless scheme is to employ the systematic Raptor design. The description of the systematic Raptor codes and their construction can be found in [4], whereas a practical implementation of systematic Raptor codes, adopted in Multimedia Broadcast/Multicast Services (MBMS) within 3GPP, is described in [10].

The combined IR-HARQ scheme B, based on the systematic Raptor design, also uses the random puncturing of a high-rate mother LDPC code as its first stage. At the receiver, after the decoding of mother LDPC code has failed, the output bits of the systematic Raptor code are transmitted which encode the information sequence via the intermediate symbols, such that Raptor decoding process can be performed using all already received symbols as well. The Raptor decoding process is then performed to decode for the intermediate symbols, by using the same procedure as presented in Section II. Block diagram for proposed combined scheme B is depicted in 4.

The decoding graph that depicts the entire decoding process is presented in Fig. 5. At first, standard sum-product decoding is performed on the mother code (far-right part of the graph). After the reception of the entire mother codeword and a number of Raptor encoding symbols, all the available soft information is used in order to calculate the LLRs of the intermediate symbols for the systematic Raptor code (middle part of the graph). Furthermore, these LLRs are additionally updated by the static precode decoding (far-left part of the graph) after a fixed number of iterations. Successful decoding of the intermediate symbols at the decoder is equivalent to successful decoding of the original information sequence, since decoder only needs to process the intermediate symbols with the first k rows of the LT generator matrix in order to obtain the information sequence. Note that in this design, the precode and the mother code need not be the same codes.

Certain inefficiency attached to combined scheme B compared to the rateless IR-HARQ scheme arises from the fact that the parity symbols of the mother code are essentially artificially embedded into the graph, and their degrees are not distributed with respect to the good output degree distribution Ω . Hence, there is a tradeoff between the mother code rate and the performance of the systematic Raptor code that follows

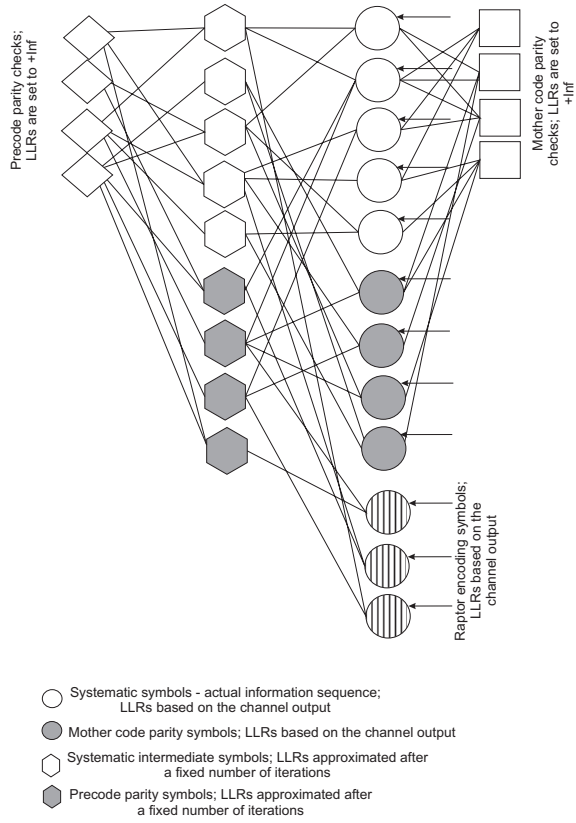


Fig. 5. Decoding graph for combined scheme B

the mother code. With a properly designed lower rate mother code, the threshold will be lower, i.e., we can have the nearly optimal performance of LDPC-based IR-HARQ at the wider region of (high) SNR, however, inefficiency introduced to the systematic Raptor scheme will be greater due to the presence of more “artificial” parity nodes, after the LDPC decoding fails.

Another issue concerning the parity symbols of the mother code embedded into the Raptor encoding symbols is the significant increase in complexity due to the large degree of the corresponding nodes in the decoding graph. Embedding of the vector of parities \mathbf{z} of the mother code of length $n - k$, into a systematic Raptor decoding graph is done using relations $\mathbf{z} = \mathbf{P}\mathbf{x}$, where $\mathbf{G}_m = [\mathbf{I}_k | \mathbf{P}^T]^T$ is the systematic form of the generator matrix of the mother code and $\mathbf{x} = \mathbf{G}_{LT}^{\{1:k\}} \bar{\mathbf{x}}$, where $\mathbf{G}_{LT}^{\{1:k\}}$ are the first k rows of the overall LT generator matrix, \mathbf{x} is the precoded information sequence and $\bar{\mathbf{x}}$ is the vector of the intermediate symbols. Thus, the adjacency matrix of the decoding graph in the combined scheme B has the form

$$\mathbf{M} = [\mathbf{H}_{pc}^T | (\mathbf{G}_{LT}^{\{1:k\}})^T | (\mathbf{P} \cdot \mathbf{G}_{LT}^{\{1:k\}})^T | (\mathbf{G}_{LT}^{\{k+1:\bar{n}\}})^T]^T. \quad (8)$$

Here, \mathbf{H}_{pc} is the parity-check matrix of the Raptor precode and $\mathbf{G}_{LT}^{\{k+1:\bar{n}\}}$ is formed by the remaining $\bar{n} - k$ rows of the overall LT generator matrix ($\bar{n} - k$ is the number of received Raptor encoding symbols). While both matrices \mathbf{P} and $\mathbf{G}_{LT}^{\{1:k\}}$ can easily be made sparse, their product $\mathbf{P} \cdot \mathbf{G}_{LT}^{\{1:k\}}$

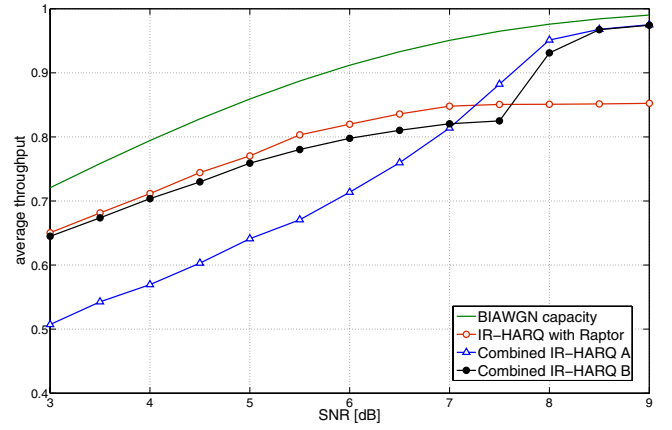


Fig. 6. Simulation results for combined scheme B

is generally not sparse. In our simulation scenario, while other Raptor encoding symbols have average degree of less than 5, the average degree of the embedded mother code parities is more than 400. Even if we neglect this, the combined scheme B would still have higher complexity since it involves three stages of decoding plus an additional LT encoder processing to derive information sequence from the intermediate symbols. Also, systematic Raptor design requires significant amount of preprocessing and Gaussian elimination to be performed at the encoder in order to calculate the intermediate symbols at the transmission of each block. However, it should be noted that all these stages of the encoding/decoding process can be, in principle, implemented in linear time [10].

The simulation results for the combined scheme B and the comparison with the corresponding rateless IR-HARQ scheme with Raptor code and combined scheme A over the BIAWGN channel are shown in Fig. 6. The Systematic Raptor code used in the simulation was implemented based on application layer Forward Error Correction (FEC) scheme described in [10] with the length of information sequence set to $k = 3140$. For fair comparison, non-systematic Raptor code used for scheme A was modified to have the same precode and the same output symbol degree distribution as its systematic version from [10]. Combined scheme B successfully takes advantage of the first part of the protocol, i.e., of puncturing the high-rate mother code, to achieve high throughput performance at the region of high SNR and also approaches the performance of Raptor IR-HARQ scheme as the SNR decreases. It significantly outperforms combined scheme A when signalling at the poor channel conditions. However, some inefficiency is induced at the SNR region around which the mother LDPC code protection starts to fail. This is due to the fact that the decoding is then performed on a different graph and the Systematic Raptor code needs a significant number of additional Raptor encoding symbols to successfully decode because it cannot make the proper use of the “artificial” encoding symbols. However, constructions of the joint design of the mother code and the LT generator matrix may exist such that the resulting degrees of the mother code parities in the new decoding graph

behave as they were actual Raptor encoding symbols. This would remove the deterioration in performance and also solve the problem of the increase in complexity induced by the embedding of the mother code parities in the new decoding graph.

V. CONCLUSION

We have constructed two combined IR-HARQ schemes with the elements of both previously studied punctured and rateless IR-HARQ schemes [5]. It has been demonstrated that these schemes achieve a nearly optimal average throughput at the high SNR region, while attaining the property of ratelessness and being able to withstand the severe channel conditions.

ACKNOWLEDGMENT

The authors would like to acknowledge the generous support of Toshiba Research Europe Ltd Telecommunications Research Laboratory in Bristol.

REFERENCES

- [1] S. Kallel, D. Haccoun, "Generalized type II hybrid ARQ scheme using punctured convolutional coding," *IEEE Transactions on Communications*, vol. 38, No. 11, pp. 1938–1946, Nov. 1990.
- [2] J. Li and K. Narayanan, "Rate-compatible low density parity check codes for capacity-approaching ARQ schemes in packet data communications," *Proc. of the Int. Conf. on Comm., Internet, and Info. Tech. (CIIT)*, Nov. 2002.
- [3] M. Luby, "LT codes," *Proc. of the 43rd Annual IEEE Symp. Foundations of Computer Science (FOCS)*, Vancouver, Canada, Nov. 2002.
- [4] A. Shokrollahi, "Raptor codes," *IEEE Transactions on Information Theory*, vol. 52, No. 6, pp. 2551–2567, June 2006.
- [5] E. Soljanin, N. Varnica, P. Whiting, "Incremental redundancy Hybrid ARQ with LDPC and Raptor codes", submitted to *IEEE Transactions on Information Theory*.
- [6] O. Etesami, A. Shokrollahi, "Raptor codes on binary memoryless symmetric channels," *IEEE Transactions on Information Theory*, vol. 52, no. 5, pp. 2033–2051, May 2006.
- [7] Q. Xu, V. Stanković, Z. Xiong, "Distributed source-channel coding of video using Raptor codes," *IEEE Journal on Selected Areas in Communications*, vol. 25, pp. 851–861, May 2007.
- [8] D.J.C. MacKay, "Encyclopedia of Sparse Graph Codes," code 3584.5.3.4326, <http://www.inference.phy.cam.ac.uk/mackay>.
- [9] M. Ardakani, F.R. Kschischang, "A more accurate one-dimensional analysis and design of irregular LDPC codes", *IEEE Transactions on Communications*, vol. 52, no. 12, pp. 2106–2114, December 2004.
- [10] 3GPP TS 26.346 V7.0.0, Technical Specification Group Services and System Aspects; Multimedia Broadcast/Multicast Service; Protocols and Codecs, December 2005.